Supplement of "Enhanced Moisture Delivery into Victoria Land, East Antarctica During the Early Last Interglacial: Implications for West Antarctic Ice Sheet Stability"

Yuzhen Yan[1,2], Nicole E. Spaulding[3], Michael L. Bender[1,4], Edward J. Brook[5], John A. Higgins[1], Andrei V. Kurbatov[3], Paul A. Mayewski[3]

[1]Department of Geosciences, Princeton University, Princeton NJ 08544, USA
[2]Department of Earth, Environmental and Planetary Sciences, Rice University, Houston TX 77005, USA
[3]Climate Change Institute, University of Maine, Orono ME 04469, USA
[4]School of Oceanography, Shanghai Jiao Tong University, Shanghai 200240, China
[5]College of Earth, Ocean, and Atmospheric Sciences, Oregon State University, Corvallis OR 97331, USA

***Correspondence to*: Yuzhen Yan (yuzhen.yan@rice.edu)**

Supplementary Text

Supplementary Figure (S1-S6)

Supplementary Data Table (1-4; uploaded as separate files)

Here, we describe how the uncertainties associated with the S27 gas chronology, the ice chronology, and Δage age are estimated.

1 S27 gas age uncertainties

Recall Equation (2) in the main text, in which we built the following function:

$$\zeta(t) = \delta^{18}O_{atm(t),\,S27} - \delta^{18}O_{atm(t),\,EDC} \quad \text{(S1)}$$

Note the $\delta^{18}O_{atm(t),\,EDC}$ is linearly interpolated between discrete analyses. The benefit of expressing synchronization in the form of Equation (S1), instead of simply asking at what time (t) $\delta^{18}O_{atm(t),\,S27} = \delta^{18}O_{atm(t),\,EDC}$, is that uncertainties can be rigorously defined and quantitatively calculated. The final chronology uncertainty has three components as discussed separately below.

1.1 Analytical uncertainties associated with $\delta^{18}O_{atm}$

S27 and EDC $\delta^{18}O_{atm}$ are independent variables. As a result, the uncertainty of $\zeta(t)$ is given by:

$$\sigma_\zeta = \sqrt{\sigma_{S27}^2 + \sigma_{EDC}^2} \quad \text{(S2)}$$

where σ_{EDC} is the pooled standard deviation of the EDC $\delta^{18}O_{atm}$ data (0.028 ‰; Extier et al, 2018) and σ_{S27} is 0.046 ‰. Taking 0.028 ‰ and 0.046 ‰ into Equation (S2), the integrated uncertainty (1σ) for $\zeta(t)$ is 0.054 ‰. Because each depth has two duplicates, the width of 95 % confidence interval (CI) of $\zeta(t)$ is ±0.076 ‰ (calculated as 0.054 ‰ multiplied by 2, and then divided by the square root of 2) assuming a Gaussian distribution.

1.2 Age uncertainties relative to the EDC chronology

In order to translate the integrated analytical uncertainties (±0.076 ‰) into age uncertainties, we repeat the direct matching process described in the main text. This time, however, we attempt to link the highest and lowest value of the 95 % CI of each S27 $\delta^{18}O_{atm}$ datum (that is, $\delta^{18}O_{atm(t),\,S27} \pm 0.076$ ‰) to the $\delta^{18}O_{atm(t),\,EDC}$ series. 28 out of the 51 samples whose age was assigned by direct matching have their age uncertainties determined this way (marked as "95 % CI directly matched" in Supplementary Data Table 3). The age uncertainties of the remaining 55 points were interpolated from the nearby age points that were successfully assigned age uncertainties via direct matching (Figure 3). Here, ice stratigraphy puts an implicit constraint on how age uncertainties could vary with depth.

1.3 Uncertainties in EDC chronology

The chronology of EDC reported by Extier et al (2018) is AICC2012, the most up-to-date and internally consistent chronology derived from multiple Antarctic ice cores (Veres et al, 2013; Bazin et al, 2013). AICC2012 has its own dating uncertainties,

which are independent from the uncertainties arising from the $\delta^{18}O_{atm}$ analyses. We thus combined these two types of uncertainties quadratically, similar to Equation (S2), and separately calculated the lower and upper bound of the 95 % confidence interval for the final absolute gas chronology.

2 S27 ice age uncertainties

Since no uncertainty estimate is available for the ice chronology established in Spaulding et al (2013), we calculate the uncertainties associated with δD_{ice} synchronization here. Similar to the case of gas chronology, the absolute uncertainty of the ice chronology consists of (1) the analytical errors in δD_{ice}, (2) age errors in S27 ice chronology relative to the EDC ice chronology, and (3) the intrinsic uncertainties of the EDC ice chronology itself.

Because S27 δD_{ice} was measured in large numbers with high analytical precision (±0.05 ‰; Spaulding et al, 2013), we expect minimal analytical errors for the ice chronology. Second, δD_{ice} tie-points chosen by Spaulding et al (2013) are clearly defined geometrical features (peaks or troughs) that allow unequivocal matching. As a result, the final uncertainty of the S27 ice chronology must be dominated by the uncertainties of the EDC chronology (AICC2012). We therefore assign the ice age uncertainty of a given EDC age point to the coeval S27 age point.

3 Δage uncertainties

Now that gas and ice chronologies are independently constructed, we evaluate the uncertainties for the Δage, which affect accumulation rate estimates. Here, the absolute ice and gas age uncertainties cannot be simply combined quadratically, because the gas age and ice age are not independent. For example, the AICC2012 gas age scale is constructed on the basis of a model-based ice scale and lock-in depth (LID) estimate, unless the gas age is synchronized via stratigraphic links (Veres et al, 2013; Bazin et al, 2013).

The uncertainty associated with S27 Δage has three components: the uncertainty of EDC Δage (which is associated with the lock-in depth), the relative uncertainty of S27 ice age to EDC ice age, the relative uncertainty of S27 gas age to EDC gas age. The Δage uncertainty in the EDC timescale is not reported explicitly. Instead, the reported uncertainty in the final AICC2012 chronology for each depth is the maximum of the gas and ice uncertainty (Bazin et al, 2013). Because there is no feasible way to evaluate the EDC Δage uncertainty, our focus here becomes the relative errors of S27 to the EDC chronologies. The relative errors apply to both the gas and ice chronologies. However, we emphasize that the true errors must be larger than what is calculated here, depending on the magnitude of the intrinsic Δage uncertainties in the AICC2012 timescale. Because δD_{ice} tie-point matching as discussed above is achieved with much higher precision than is possible with $\delta^{18}O_{atm}$ synchronization, we assume that Δage uncertainties to equal the gas age uncertainties of S27 relative to EDC.

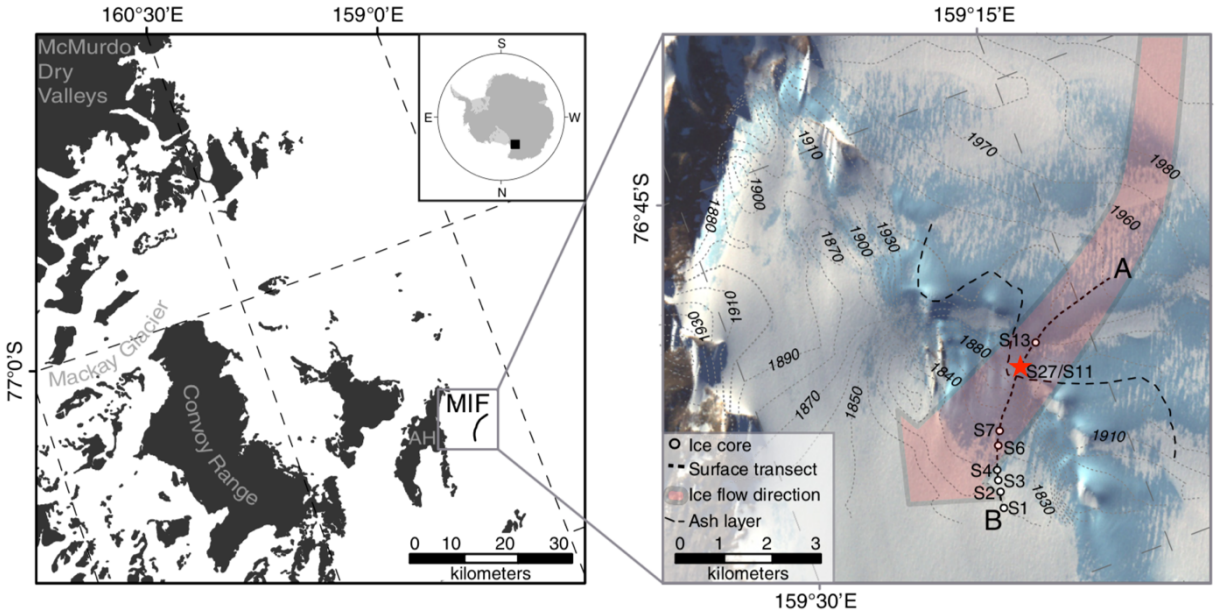

Figure S1: Geographic settings of the Allan Hills area (left) and the location of S27 ice cores (red star), modified after Spaulding et al (2013). Also shown on the right panel are a series of surface ice samples collected on the transect marked by the dashed line between A and B as well as shallow ice cores from S1 to S27. The red arrow shows the measured ice flow according to Spaulding et al (2012). Thin dashed lines mark the local elevation. The ash layer intercepting the transect A-B at S27 is one of the many ash layers used as an age reference point. Copyright © University of Washington.

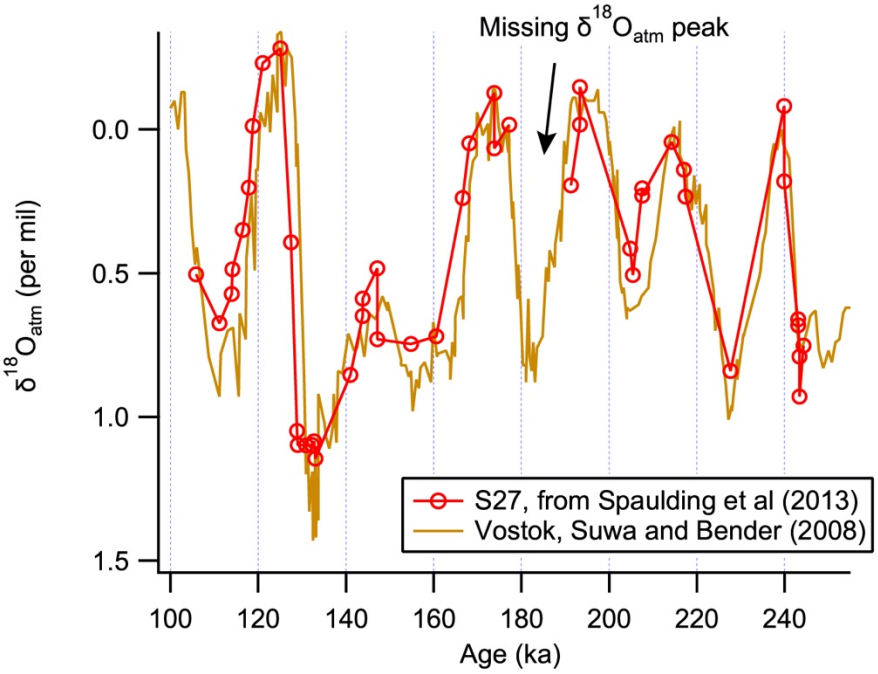

Figure S2: $\delta^{18}O$ of paleo-atmospheric O_2 ($\delta^{18}O_{atm}$) measurements from S27 (red) reported in Spaulding et al (2013) in comparison with the same property measured in Vostok (brown) by Suwa and Bender (2008). The location of the missing $\delta^{18}O_{atm}$ peak from ~180 ka from earlier measurements is indicated by the black arrow.

Depth <148 m:

2013: $\delta O_2/N_2$ (‰) = -0.0317*depth (m) - 8.79; 2018: $\delta O_2/N_2$ (‰) = -0.0360*depth (m) - 10.95

Depth >148 m:

2013: $\delta O_2/N_2$ (‰) = -0.205*depth (m) - 24.26; 2018: $\delta O_2/N_2$ (‰) = -0.106*depth (m) - 0.37

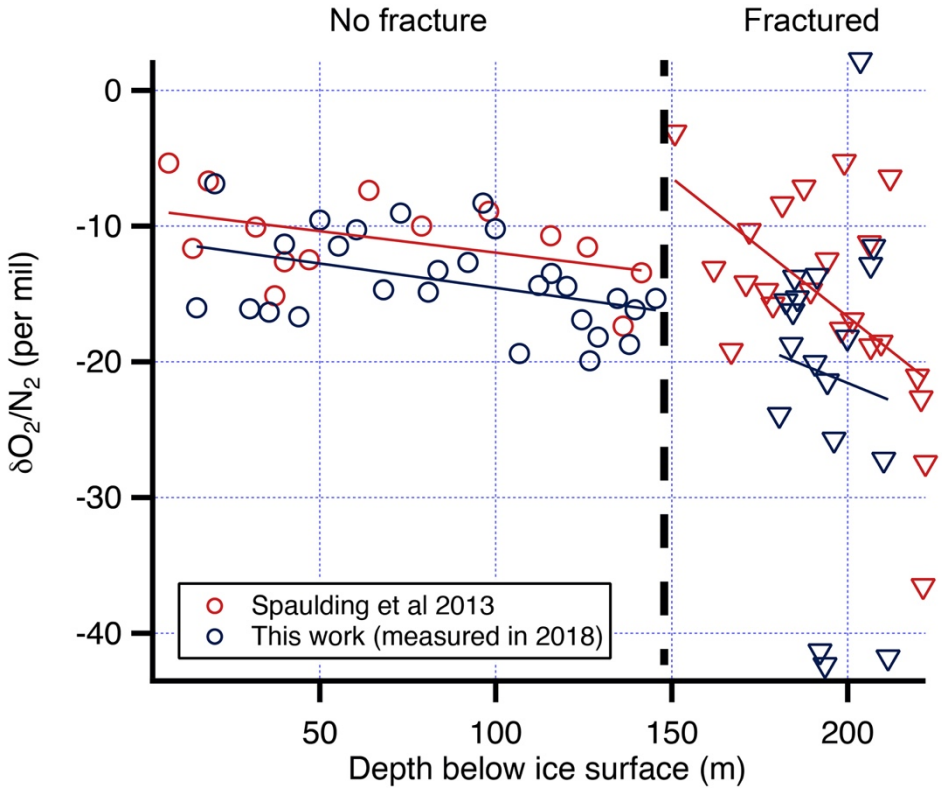

Figure S3: Depletion of $\delta O_2/N_2$ due to gas loss after five years in S27. $\delta O_2/N_2$ data points shown in red are from data measured in 2013, and $\delta O_2/N_2$ in dark blue were measured in 2018. Circles indicate $\delta O_2/N_2$ measurements on ice without any visible fracture, whereas triangles represent $\delta O_2/N_2$ measured on heavily fractured ice. The preferential loss of O_2 relative to N_2 is revealed by the lowered trend line (where $\delta O_2/N_2$ is regressed against depth). This offset in $\delta O_2/N_2$ is assumed to be depth-dependent and subsequently used in the gas loss correction. Note that new and earlier gas measurements were not carried on the exact same depth. The break in the lines at 148 m depth is arbitrary. It is the average depth of the deepest sample with good core quality (no fracture) and the shallowest fractured sample. The data could be represented by unbroken lines as well. However, given that the slope of $\Delta\delta^{18}O_{grav}$ vs. $\Delta\delta O_2/N_2$ is only 0.007 ‰ ‰$^{-1}$ (Figure S4), the choice of regression lines here will have only a small impact on the subsequent data and analysis.

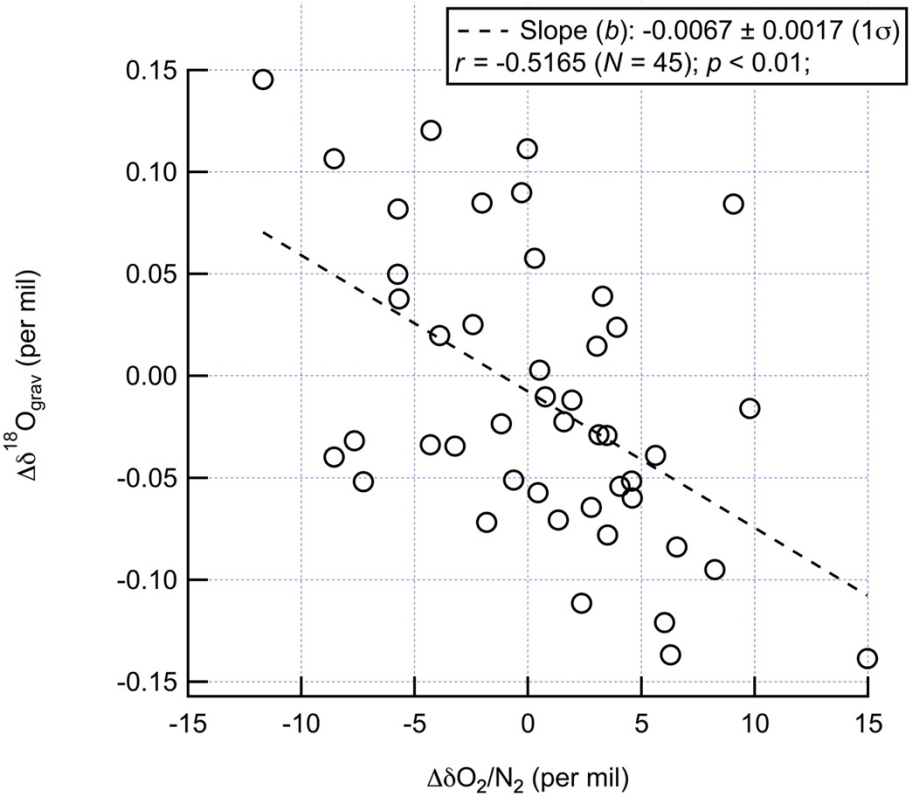

90

Figure S4: Impact on $\delta^{18}O_{atm}$ due to gas loss in S27. The difference in the elemental and isotopic compositions between two replicates is attributable to gas loss. The slope of the regression line, *b*, of replicate $\delta^{18}O_{grav}$ differences on replicate $\delta O_2/N_2$ differences is used to correct for gas losses according to Equation (1) in the main text. The magnitude of final gas loss correction is typically ~0.020 ‰.

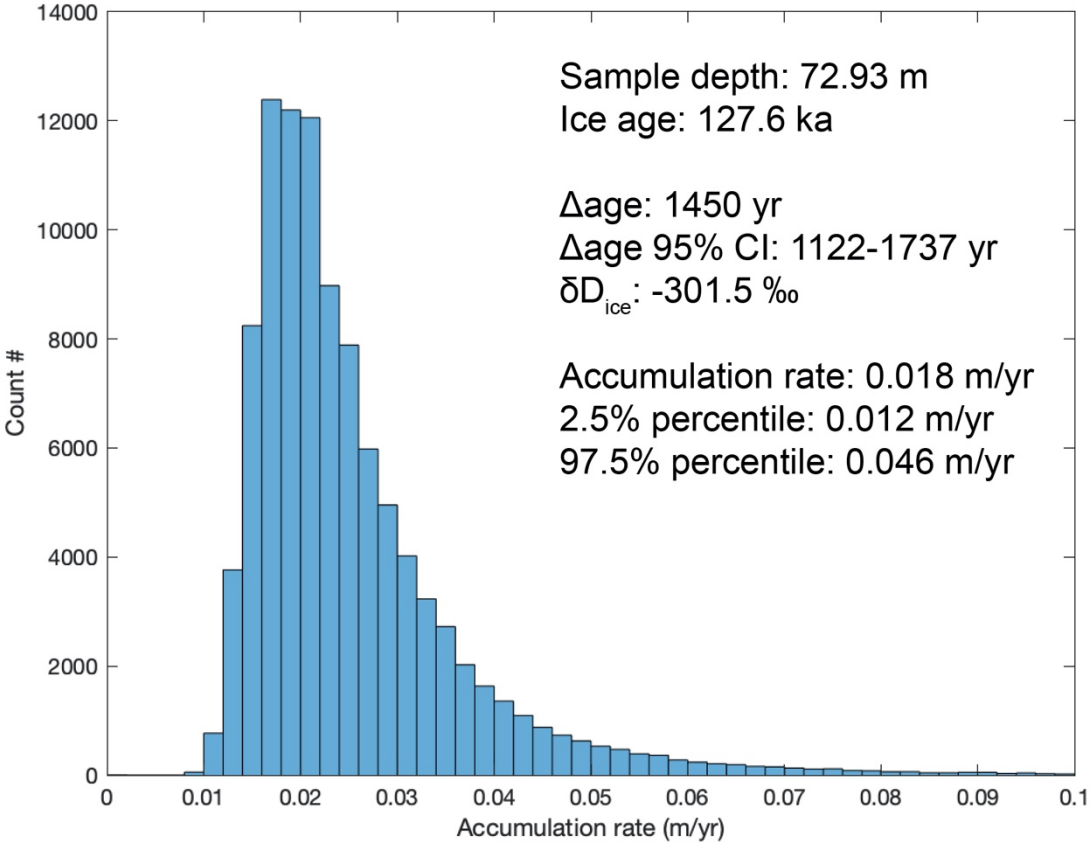

Figure S5: An example of the Monte Carlo simulation used to estimate the distribution of accumulation rates given known Δage and δD_{ice} values. The spread originates from the uncertainties in Δage. For each Δage datum, simulations are run 100,000 times to compute the probability distribution of accumulation rates. The mode of the 100,000 runs is reported as the accumulation rate corresponding to that Δage. Note that because the data is not normally distributed, taking the arithmetic average of the 100,000 estimated values would lead to apparent overestimation. To quantify uncertainties associated with the accumulation rate estimate, 2.5% and 97.5 % percentile values are taken as the lower and upper limits of the 95% confidence interval (CI), respectively. The final reported accumulation rate for this datum with a Δage of 1450 yr (95% CI: 1122-1737 yr) at 127.6 ka is 0.018 m yr^{-1} (95% CI: 0.012-0.046 m yr^{-1}).

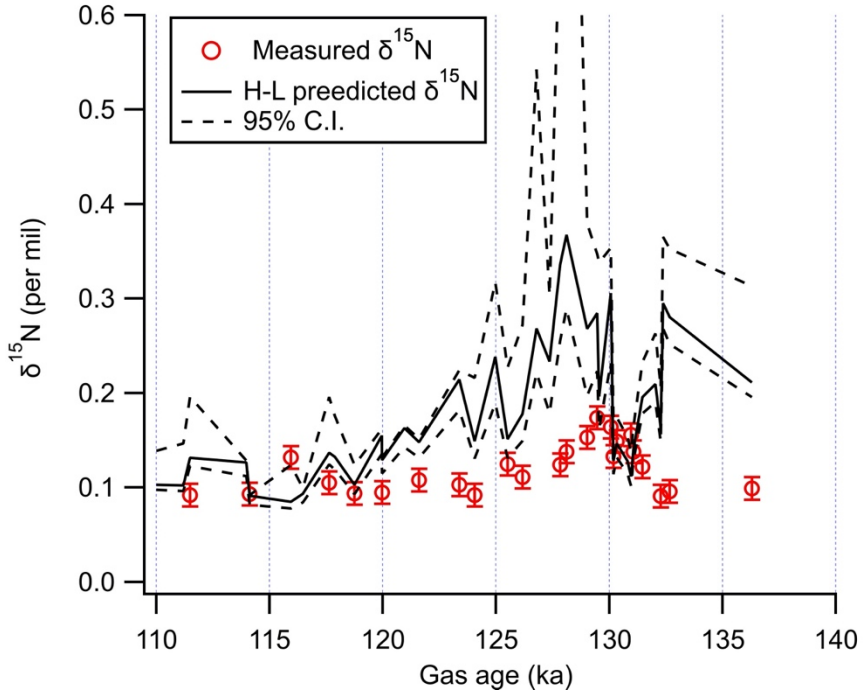

Figure S6: $\delta^{15}N$ values estimated from the H-L model (black) and measured in S27 ice (red). Dashed lines represent the 95% confidence interval (C.I.) of the model-predicted $\delta^{15}N$. Error bar associated with measured $\delta^{15}N$ values represent pool standard deviation of $\delta^{15}N$ measurements (0.012 ‰). When using the H-L model to predict $\delta^{15}N$, we assumed the height of the lock-in zone to be 3 m, and the height of convective zone to be 0 m

References

Bazin, L., Landais, A., Lemieux-Dudon, B., Kele, H.T.M., Veres, D., Parrenin, F., Martinerie, P., Ritz, C., Capron, E., Lipenkov, V. and Loutre, M.F.: An optimized multi-proxy, multi-site Antarctic ice and gas orbital chronology (AICC2012): 120-800 ka, Clim. Past, 9, 1715-1731, https://doi.org/10.5194/cp-9-1715-2013, 2013.

Extier, T., Landais, A., Bréant, C., Prié, F., Bazin, L., Dreyfus, G., Roche, D.M. and Leuenberger, M.: On the use of $\delta^{18}O_{atm}$ for ice core dating, Quaternary Sci. Rev., 185, 244-257, https://doi.org/10.1016/j.quascirev.2018.02.008, 2018.

Spaulding, N.E., Higgins, J.A., Kurbatov, A.V., Bender, M.L., Arcone, S.A., Campbell, S., Dunbar, N.W., Chimiak, L.M., Introne, D.S. and Mayewski, P.A.: Climate archives from 90 to 250 ka in horizontal and vertical ice cores from the Allan Hills Blue Ice Area, Antarctica, Quaternary Res., 80, 562-574, https://doi.org/10.1016/j.yqres.2013.07.004, 2013.

Spaulding, N.E., Spikes, V.B., Hamilton, G.S., Mayewski, P.A., Dunbar, N.W., Harvey, R.P., Schutt, J. and Kurbatov, A.V.: Ice motion and mass balance at the Allan Hills blue-ice area, Antarctica, with implications for paleoclimate reconstructions, J. Glaciol., 58, 399-406, https://doi.org/10.3189/2012JoG11J176, 2012.

Suwa, M. and Bender, M.L.: Chronology of the Vostok ice core constrained by O_2/N_2 ratios of occluded air, and its implication for the Vostok climate records, Quaternary Sci. Rev., 27, 1093-1106, https://doi.org/10.1016/j.quascirev.2008.02.017, 2008.

Veres, D., Bazin, L., Landais, A., Toyé Mahamadou Kele, H., Lemieux-Dudon, B., Parrenin, F., Martinerie, P., Blayo, E., Blunier, T., Capron, E. and Chappellaz, J.: The Antarctic ice core chronology (AICC2012): an optimized multi-parameter and multi-site dating approach for the last 120 thousand years, Clim. Past, 9, 1733-1748, https://doi.org/10.5194/cp-9-1733-2013, 2013.